Multiscale Theory of Fluctuating Interfaces: Renormalization of Atomistic Models

Christoph A. Haselwandter and Dimitri D. Vvedensky
The Blackett Laboratory, Imperial College, London SW7 2BW, United Kingdom
(Received 29 November 2005; published 23 January 2007)

We describe a framework for the multiscale analysis of atomistic surface processes which we apply to a model of homoepitaxial growth with deposition according to the Wolf-Villain model and concurrent surface diffusion. Coarse graining is accomplished by calculating renormalization-group (RG) trajectories from initial conditions determined by the regularized atomistic theory. All of the crossover and asymptotic scaling regimes known from computer simulations are obtained, but we also find that two-dimensional substrates show an intriguing transition from smooth to mounded morphologies along the RG trajectory.

DOI: 10.1103/PhysRevLett.98.046102 PACS numbers: 81.15.Aa, 05.10.Gg

Nonequilibrium phenomena in many settings are modeled by lattice gases with transition rules designed to capture the essence of atomic-scale interactions [1,2]. Our interest here is in the morphologies of fluctuating interfaces driven by the deposition of new material. Given an atomistic model for an experimental scenario, there are, broadly speaking, two standard modelling methodologies. The first is to perform kinetic Monte Carlo (KMC) simulations, which yield a description of morphological evolution that is amenable to direct comparison with experiments [3–5]. The second approach is based on postulating a coarse-grained Langevin equation for the system [6]. The properties of this equation can then be ascertained either by numerical integration or with analytic methods used in statistical dynamics [6–10].

In this Letter, we derive stochastic differential equations directly from the rules of lattice models. We first obtain lattice Langevin equations that embody the transition rules of atomistic models [11,12]. This formulation is the starting point for coarse graining in that the associated regularized equations provide initial conditions for a dynamic renormalization-group (RG) analysis. The points along the RG trajectories correspond to hierarchies of equations that describe atomistic models over expanding length and time scales. These ideas establish a general framework for the multiscale analysis of nonequilibrium systems.

For ease of exposition, we describe our method for a one-dimensional (1D) substrate. We have a lattice of length L on each site i of which is a column whose topmost particle is at height H_i. Every surface profile corresponds uniquely to an array $\mathbf{H} = \{H_1, H_2, \ldots, H_L\}$. The system evolves according to the Chapman-Kolmogorov equation [13] for the transition probability $T_{t+t'}(\mathbf{H}_3|\mathbf{H}_1)$ from configuration $\mathbf{H}_1$ to $\mathbf{H}_3$ in the time interval $t + t'$,

$$T_{t+t'}(\mathbf{H}_3|\mathbf{H}_1) = \sum_{\mathbf{H}_2} T_{t'}(\mathbf{H}_3|\mathbf{H}_2) T_t(\mathbf{H}_2|\mathbf{H}_1), \qquad (1)$$

where $t = t_2 - t_1$ and $t' = t_3 - t_2$. This equation is an identity satisfied by all Markov processes and is the definitive statement of the evolution of our lattice model. A familiar special case is the master equation.

The Chapman-Kolmogorov equation can be transformed into a more analytically tractable form by carrying out a Kramers–Moyal–van Kampen expansion [12] to obtain the lattice Langevin equation

$$\frac{dh_i}{d\tau} = K_i^{(1)} + \eta_i, \qquad (2)$$

where h_i and τ are continuous height and time variables, $K_i^{(1)}$ is the first moment of the transition rate density, and the η_i are Gaussian noises that have zero mean and covariances $\langle \eta_i(\tau)\eta_j(\tau')\rangle = K_{ij}^{(2)}\delta(\tau - \tau')$, in which $K_{ij}^{(2)}$ is the second moment of the transition rate density and $\delta(x)$ is the Dirac delta function. The transition moments are defined by

$$K_i^{(1)}(\mathbf{h}) = \int r_i W(\mathbf{h};\mathbf{r}) d\mathbf{r}, \qquad (3)$$

$$K_{ij}^{(2)}(\mathbf{h}) = \int r_i r_j W(\mathbf{h};\mathbf{r}) d\mathbf{r}, \qquad (4)$$

where $W(\mathbf{h};\mathbf{r})$ is the transition rate density from $\mathbf{h}$ to $\mathbf{h} + \mathbf{r}$, and $\mathbf{r}$ is the array of jump lengths. W is determined by applying the transition rules to each height configuration that is resolved by the model.

We illustrate our method for homoepitaxial growth, wherein new material is deposited onto a crystalline surface of the same material, with concurrent surface diffusion, and eventual incorporation into the growing crystal. At temperatures too low for activated surface diffusion, ordered growth can still occur [14] because of short-range nonthermal motion of newly deposited species to increase their coordination [15,16]. Examples of this effect are transient mobility [15–17], ballistic impact [18,19], and downward funneling [20]. A basic description of such processes is provided by the Wolf-Villain (WV) model [21,22]. The transition rules of this model stipulate that a particle arriving at a randomly chosen site remains there only if its coordination cannot be increased by moving to a

nearest neighbor site. Otherwise, the deposition site is chosen randomly from nearest neighbor sites that offer the maximum coordination.

Thermally activated diffusion is modeled as the nearest neighbor hopping of surface particles according to an Arrhenius rate [23] $\nu_0 e^{-\beta E}$, where $\nu_0 \sim 10^{13}$ s^{-1}, $\beta = 1/(k_B T)$, k_B is Boltzmann's constant, T is the absolute temperature, and E is the energy barrier to hopping. We take [5,11] $E = E_S + n_i E_N$, where E_S is the energy barrier from the substrate and E_N is the contribution from each of the n_i lateral nearest neighbors. By combining these diffusion rates with the WV model for deposition, we obtain a prototype lattice model for homoepitaxial growth [24]. For 1D substrates, our model resolves 40 configurations, but for two-dimensional (2D) substrates, this number explodes to 126 192. The generation and manipulation of these configurations to evaluate Eqs. (3) and (4) are achieved with MATHEMATICA [25].

The only remaining implementation issue arises from the passage from discrete heights in Eq. (1) to the continuous heights in Eq. (2). The comparison of nearest neighbor heights to determine the coordination, e.g., $n_i = \theta(h_{i-1} - h_i) + \theta(h_{i+1} - h_i)$ for 1D substrates, is based on the step function θ, defined by $\theta(N) = 1$ if $N \geq 0$ and $\theta(N) = 0$ if $N < 0$ for integer N. For continuous heights, θ must be represented by a continuous function. We use

$$\theta(\Delta h; \delta) = \frac{1}{2} \int_{-\infty}^{\Delta h} [\mathrm{erf}((s+1)\delta) - \mathrm{erf}(s\delta)] ds, \qquad (5)$$

where $\delta > 0$ and erf is the error function. Note that $\lim_{\delta \to \infty} \theta(N; \delta) = \theta(N)$. With this proviso for θ, Eq. (2) provides an extension of our original lattice model defined by Eq. (1) to continuous height and time variables [12].

The foregoing analytic formulation is the starting point for coarse graining the atomic-scale equations (2)–(4). We introduce the continuous spatial variable x and the analytic height function $u(x, \tau)$. The substitution of the Taylor expansions of u and θ into Eqs. (2)–(4) yields a convergent series with successively higher spatial derivatives of u. Figure 1 shows that for $\delta > 1$, the roughness curves obtained from the lattice equation (2) and KMC simulations of the WV model are in excellent agreement. This suggests that a large-order continuum equation would accurately describe the atomistic dynamics. For small δ, however, only terms that determine fundamental properties of the lattice model, such as the scaling behavior, are retained [Fig. 1 (inset)], and we find

$$\frac{\partial u}{\partial \tau} = \nu_2 \nabla^2 u - \nu_4 \nabla^4 u + \lambda_{13} \nabla (\nabla u)^3 + \lambda_{22} \nabla^2 (\nabla u)^2 + \xi, \qquad (6)$$

where the smoothed Gaussian noise ξ has zero mean and covariance $\langle \xi(\mathbf{x}, \tau) \xi(\mathbf{x}', \tau') \rangle = 2\mathcal{D} \delta(\mathbf{x} - \mathbf{x}') \delta(\tau - \tau')$, with $\mathcal{D} = D_0 - D_2 \nabla^2$. The leading-order equation (6) is obtained if the order of the dominant terms does not decrease as the coarse graining of height differences

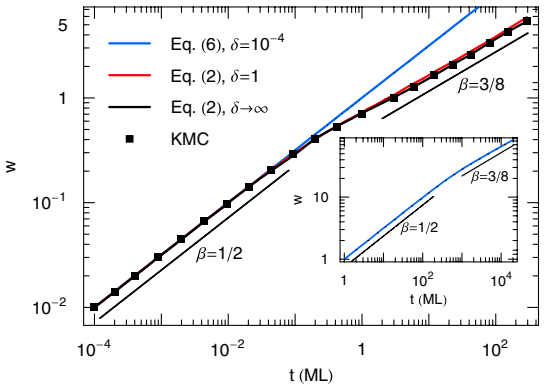

FIG. 1 (color online). Roughness $w \equiv [\langle h^2(t) - \langle h(t) \rangle^2 \rangle]^{1/2}$ versus time, measured in monolayers (ML) deposited, for the 1D WV model with $L = 40000$ computed from KMC simulations and solutions of the lattice equation (2) for the indicated values of δ, and the continuum equation (6) with the coefficients in Table I (inset). Individual data sets were obtained from single realizations. Lines with slopes $\beta = 1/2$ and $\beta = 3/8$, consistent with random deposition and the Mullins-Herring equation, respectively, are shown for comparison [34].

through Eq. (5) increases. This places an upper bound on δ, but the numerical value of δ is not too crucial, provided it lies below this upper bound. The values of the coefficients in Eq. (6) for the WV model are compiled in Table I. Surface diffusion modifies the values only of ν_4, λ_{22}, and D_2. Their expressions, which involve the model parameters and the substrate dimension, will be reported elsewhere.

The derivation of the leading-order continuum equation (6) relies on the expansion of Eq. (2) as a convergent Taylor series. There are models for which higher-order terms must be retained, for example, for reasons of stability [26]. But there are also scenarios [27] where the form of the continuum equation suggests that an altogether different approach might be required. Such cases will be reserved for future investigations.

The general form of Eq. (6) has been previously postulated on the basis of symmetry arguments and subsumes several widely studied equations of conserved surface growth [6]: the Edwards-Wilkinson (EW) equation, $u_\tau = \nu_2 \nabla^2 u + \xi$, the Mullins-Herring (MH) equation, $u_\tau = -\nu_4 \nabla^4 u + \xi$, and the Villain–Lai–Das Sarma (VLDS) equation, $u_\tau = -\nu_4 \nabla^4 u + \lambda_{22} \nabla^2 (\nabla u)^2 + \xi$, where the noise ξ may be conserved ($D_0 = 0$) or nonconserved ($D_2 = 0$). The justification of such equations for particular growth scenarios typically relies on phenomenological and

TABLE I. Rounded coefficients in Eq. (6) for the WV model with substrate dimension d. The values are obtained with the representative choices $\delta = 10^{-4}$ ($d = 1$) and $\delta = 1$ ($d = 2$).

d	ν_2	ν_4	λ_{13}	λ_{22}	D_0	D_2
1	2×10^{-9}	5×10^{-5}	-4×10^{-17}	3×10^{-9}	$\frac{1}{2}$	0
2	5×10^{-2}	1×10^{-1}	-4×10^{-2}	-4×10^{-2}	$\frac{1}{2}$	0

scaling arguments to eliminate some of the terms in Eq. (6). However, as will be shown below, even terms often regarded as being negligible, such as $\lambda_{13}\nabla(\nabla u)^3$, can play a role at longer length and time scales.

We construct differential RG equations [7] to one-loop order, which necessitates evaluating 16 Feynman-type diagrams and modifies the noise covariance to $\mathcal{D} = D_0 - D_2\nabla^2 + D_4\nabla^4$ [9]. The details of this lengthy but standard calculation will be presented elsewhere. Under the scale changes $\mathbf{x} \to e^{\ell}\mathbf{x}$, $\tau \to e^{z\ell}\tau$, and $u \to e^{\alpha\ell}u$, the coefficients in Eq. (6) renormalize according to

$$\frac{d\nu_2}{d\ell} = (z-2)\nu_2 + K_d\frac{d+2}{d}\frac{\lambda_{13}D\Lambda^d}{\nu}, \tag{7}$$

$$\frac{d\nu_4}{d\ell} = (z-4)\nu_4 - \frac{K_d}{d}\frac{\lambda_{22}^2 D_s\Lambda^d}{\nu^3}, \tag{8}$$

$$\frac{d\lambda_{13}}{d\ell} = (z-4+2\alpha)\lambda_{13} - \frac{AK_d}{d(d+2)}\frac{\lambda_{13}^2 D\Lambda^d}{\nu^2}, \tag{9}$$

$$\frac{d\lambda_{22}}{d\ell} = (z-4+\alpha)\lambda_{22} - 2K_d\frac{d+2}{d}\frac{\lambda_{13}\lambda_{22}D\Lambda^d}{\nu^2}, \tag{10}$$

$$\frac{dD_0}{d\ell} = (z-d-2\alpha)D_0, \tag{11}$$

$$\frac{dD_2}{d\ell} = (z-d-2\alpha-2)D_2, \tag{12}$$

$$\frac{dD_4}{d\ell} = (z-d-2\alpha-4)D_4 + K_d\frac{\lambda_{22}^2 D^2\Lambda^{d-2}}{\nu^3}, \tag{13}$$

where $K_d = S_d/(2\pi)^d$, $S_d = 2\pi^{d/2}/\Gamma(\frac{1}{2}d)$ is the surface area of a d-dimensional unit sphere, $A = d^2 + 6d + 20$, $\nu = \nu_2 + \nu_4\Lambda^2$, $D_s = \sum_{i=0}^{2}[(d-4+2i)\nu - 2\nu_4\Lambda^2]D_{2i}\Lambda^{2i}$, $D = D_0 + D_2\Lambda^2 + D_4\Lambda^4$, and Λ is the momentum cutoff.

To investigate crossover regimes, we define the variables

$$r = \frac{\nu_4\Lambda^2}{\nu_2 + \nu_4\Lambda^2}, \tag{14}$$

$$u_1 = K_d\frac{3d^2+14d+28}{d^2(d+2)}\frac{D_0\lambda_{13}\Lambda^d}{(\nu_2+\nu_4\Lambda^2)^2}, \tag{15}$$

$$u_2 = \left[K_d\frac{3(6-d)}{d(4-d)}\frac{D_0\lambda_{22}^2\Lambda^{d+2}}{(\nu_2+\nu_4\Lambda^2)^3}\right]^{1/2}, \tag{16}$$

$\Gamma_2 = D_2\Lambda^2/D_0$, and $\Gamma_4 = D_4\Lambda^4/D_0$, in terms of which the RG equations (7)–(13) reduce to

$$\frac{dr}{d\ell} = -2r(1-r) - 2Bru_1\Gamma + 2C(1-r)u_2^2\Gamma_s, \tag{17}$$

$$\frac{du_1}{d\ell} = u_1[-d+4r - du_1\Gamma - 4Cu_2^2\Gamma_s], \tag{18}$$

$$\frac{du_2}{d\ell} = u_2\left[-\frac{1}{2}(d+2) + 3r - 7Bu_1\Gamma - 3Cu_2^2\Gamma_s\right], \tag{19}$$

$$\frac{d\Gamma_2}{d\ell} = -2\Gamma_2, \tag{20}$$

$$\frac{d\Gamma_4}{d\ell} = -4\Gamma_4 + 2dCu_2^2\Gamma^2, \tag{21}$$

where we have used the scaling relation implied by Eq. (11) [8,9], $\Gamma = 1 + \Gamma_2 + \Gamma_4$, $\Gamma_s = 4 - d + 2r + \Gamma_2(2-d+2r) + \Gamma_4(-d+2r)$, and

$$B = \frac{d(d+2)^2}{2(3d^2+14d+28)}, \qquad C = \frac{4-d}{6(6-d)}. \tag{22}$$

There are 12 fixed points of these RG equations, of which only the EW fixed point ($r = u_i = \Gamma_j = 0$, for $i = 1, 2$ and $j = 2, 4$) is stable for $d = 1, 2, 3$. The other fixed points will be discussed elsewhere. The solution of Eqs. (17)–(21) subject to the initial conditions in Eq. (6) yields the RG trajectories of our atomistic model.

The RG trajectory of the 1D WV model (Fig. 2) shows an initial crossover from MH to VLDS behavior, followed by a crossover to the EW fixed point. The final crossover is influenced by a change in the magnitude of $u_1 \sim \lambda_{13}$. Although this term appears insignificant in the microscopic equation (Table I), it affects the coarse-grained properties of the system. This trajectory is in excellent agreement with KMC simulations [22,28], which observe the same crossover sequence, but our analytic theory also provides continuum equations for crossover regimes. Surface diffusion does not change the crossover in Fig. 2 but, for high enough temperatures, shifts the initial conditions towards the MH equation with conserved noise.

A similar transition in the initial conditions from nonconserved to conserved noise is obtained for our 2D model with increasing temperature (Fig. 3). In contrast to the 1D case, however, ν_2 changes sign along the RG trajectory, leading to the coarse-grained equation

$$\frac{\partial u}{\partial\tau} = -|\nu_2|\nabla^2 u - |\nu_4|\nabla^4 u - |\lambda_{13}|\nabla(\nabla u)^3 + \lambda_{22}\nabla^2(\nabla u)^2 + \xi. \tag{23}$$

The linearized form of this equation has a critical wave number $k_c = \sqrt{|\nu_2/\nu_4|}$ below which all modes are unstable. The maximally unstable mode $k_m = k_c/\sqrt{2}$ defines the characteristic length $2\pi/k_m$ that sets the scale for a

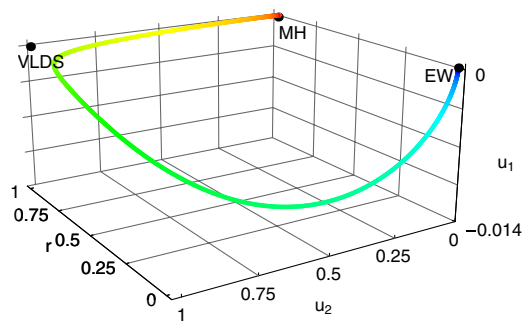

FIG. 2 (color online). RG trajectory of the 1D WV model with the initial conditions in Table I. The flow starts near the MH fixed point, crosses over to the VLDS fixed point, and then to the EW fixed point.

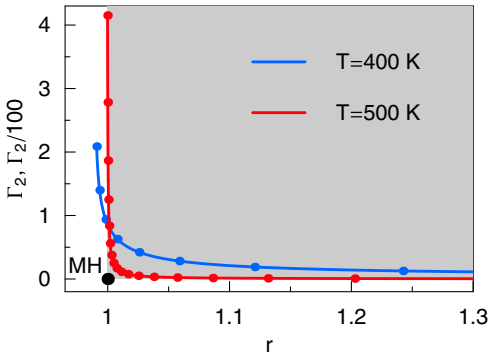

FIG. 3 (color online). RG trajectories of our 2D model obtained from Eq. (6) for two different temperatures. Superimposed on the trajectories are points separated by a logarithmic "scale" $\Delta\ell = 1/5$ [35]. The RG flow is directed towards increasing values of r, and Γ_2 is divided by 100 for the trajectory at $T = 500$ K. The shaded region corresponds to $r > 1$ and $u_2 > 0$, for which Eqs. (14) and (16) imply $\nu_2 < 0$ and $\nu_4 > 0$.

regular array of islands with diverging heights, which preempts kinetic roughening. These conclusions are consistent with large-scale computer simulations of the 2D WV model [29], where a mounded surface morphology is observed for long simulation times.

Recent low-temperature experiments on Ge(001) [30] have found a growth-mode transition leading to epitaxial breakdown. The surface morphology (see Fig. 4 of Ref. [30]) is smooth initially, but further deposition sees the emergence of a regular array of unstable mounds. This is precisely the sequence predicted in Fig. 3 for low temperatures. In the 2D WV model, particles not only jump down, which locally flattens the surface, but also up. Downward jumps dominate initially, but eventually the upward current leads to an unstable surface morphology [29]. Figure 3 suggests that at higher temperatures, surface diffusion delays this instability through an extended residence time near the MH fixed point.

In summary, we have described a multiscale method for the analysis of fluctuating interfaces that provides, beginning with atomistic processes, a hierarchy of Langevin equations across length and time scales. Striking illustrations of the effectiveness of our approach are provided by the complex crossover sequence of the 1D WV model, and by the transition from smooth to mounded surface morphologies exhibited by our 2D model. Such applications are especially pertinent for transient regimes [31–33], where the description of growth experiments in terms of phenomenological continuum equations remains problematic. The generality of our method opens the door to similar studies of other nonequilibrium systems.

This work was supported by the U.K. Engineering and Physical Sciences Research Council and the European Commission Sixth Framework Programme as part of the European Science Foundation EUROCORES Programme on Self-Organized Nanostructures (SONS).

[1] D. H. Rothman and S. Zaleski, *Lattice-Gas Cellular Automata: Simple Models of Complex Hydrodynamics* (Cambridge University Press, Cambridge, 1997).
[2] N. Gershenfeld, *The Nature of Mathematical Modelling* (Cambridge University Press, New York, 1999), Chap. 9.
[3] A. Madhukar and S. V. Ghaisas, CRC Crit. Rev. Solid State Mater. Sci. **14**, 1 (1988).
[4] H. Metiu *et al.*, Science **255**, 1088 (1992).
[5] T. Shitara *et al.*, Phys. Rev. B **46**, 6815 (1992).
[6] A.-L. Barabási and H. E. Stanley, *Fractal Concepts in Surface Growth* (Cambridge University Press, Cambridge, 1995).
[7] E. Medina *et al.*, Phys. Rev. A **39**, 3053 (1989).
[8] Z.-W. Lai and S. Das Sarma, Phys. Rev. Lett. **66**, 2348 (1991).
[9] L.-H. Tang and T. Nattermann, Phys. Rev. Lett. **66**, 2899 (1991).
[10] J. M. López *et al.*, Phys. Rev. Lett. **94**, 166103 (2005).
[11] D. D. Vvedensky *et al.*, Phys. Rev. E **48**, 852 (1993).
[12] A. L.-S. Chua *et al.*, Phys. Rev. E **72**, 051103 (2005).
[13] N. G. van Kampen, *Stochastic Processes in Physics and Chemistry* (North-Holland, Amsterdam, 1981).
[14] J. Aarts *et al.*, Appl. Phys. Lett. **48**, 931 (1986).
[15] W. F. Egelhoff, Jr. and I. Jacob, Phys. Rev. Lett. **62**, 921 (1989).
[16] S. C. Wang and G. Ehrlich, Phys. Rev. Lett. **71**, 4174 (1993).
[17] G. L. Kellogg, Phys. Rev. Lett. **76**, 98 (1996).
[18] Z. Zhang and H. Metiu, Surf. Sci. **245**, 353 (1991).
[19] C. M. Gilmore and J. A. Sprague, Phys. Rev. B **44**, 8950 (1991).
[20] J. W. Evans *et al.*, Phys. Rev. B **41**, 5410 (1990).
[21] S. Clarke and D. D. Vvedensky, Phys. Rev. B **37**, 6559(R) (1988).
[22] D. E. Wolf and J. Villain, Europhys. Lett. **13**, 389 (1990).
[23] A. Zangwill, *Physics at Surfaces* (Cambridge University Press, Cambridge, 1988).
[24] S. Clarke *et al.*, Surf. Sci. **255**, 91 (1991).
[25] Computer Code MATHEMATICA, Wolfram Research, Inc., Urbana-Champaign, IL; version 5.0.
[26] C. A. Haselwandter and D. D. Vvedensky, Phys. Rev. B **74**, 121408(R) (2006).
[27] O. Pierre-Louis *et al.*, Phys. Rev. Lett. **80**, 4221 (1998).
[28] M. Kotrla and P. Šmilauer, Phys. Rev. B **53**, 13 777 (1996).
[29] S. Das Sarma *et al.*, Phys. Rev. E **65**, 036144 (2002).
[30] K. A. Bratland *et al.*, Phys. Rev. B **67**, 125322 (2003).
[31] H.-C. Kan *et al.*, Phys. Rev. Lett. **92**, 146101 (2004).
[32] A. Ballestad *et al.*, Phys. Rev. Lett. **86**, 2377 (2001).
[33] T. Tadayyon-Eslami *et al.*, Phys. Rev. Lett. **97**, 126101 (2006).
[34] In the random deposition regime the Langevin equations yield excellent agreement with KMC simulations for any $\delta > 0$ because D_0 does not depend on δ.
[35] Close to the MH fixed point with conserved or nonconserved noise, ℓ can be easily related to τ via $z \sim 4$.